

Influence of Rear Slant Angle on Drag and Lift of the Ahmed Body

BEN MOUSSA Lamiae ^{1*}, *EL KHALFI* Ahmed ^{1†}, and *SEDDOUKI* Abbass ¹

¹Sidi Mohamed Ben Abdellah University, Faculty of Sciences and Techniques, Research Laboratory in Science and Engineering, Fez 30000, Morocco

Abstract. Through computer simulations using numerical methods, an Ahmed body model, was examined to study the aerodynamic properties, as well as the evolution of vortex patterns at the rear of this model. Tests were conducted at three different rear slant angles of 15°, 30° and 45° to evaluate the drag and lift forces. A change in the rear slant angle of the vehicle results in changes in vortex flow because vortex formation and separation adjust to this difference. The best readings for minimum drag and lift were observed on the model surface at 15°, leading to higher readings at both 30° and 45° when vortices formed. The stress points between the two surfaces move as more lift is created by strong changes in airflow near the wings at moderate to high angles of climb. The research objective is to enhance the rear design of the vehicle by finding out how to cut down on air resistance without affecting stability. The stream lines and overall flow shape were examined using ANSYS Fluent, with velocity input at 30 m/s acting as the turning condition.

Keywords: Aerodynamics, Ahmed Body, CFD, Drag reduction, Lift coefficient, rear angle.

1 Introduction

Improving vehicle performance while reducing energy consumption requires focusing on the aerodynamic performance of the vehicle. In order to analyze air flows around vehicles, the Ahmed model is used as a reference due to the simplicity of its geometry and the availability of many experimental data about it [1]. Research studies confirm that the slope of the back of an Ahmed model affects when and how the flow separates and the vortex structure is formed. Depending on the change in the angle of the rear of the vehicle, the aerodynamic forces change, which affects the vortex dynamics and the context of lift and drag forces [2].

Increasing the angles between 10° and 30° results in increased drag, due to the appearance of longitudinal swirling structures near the sides of the vehicle, where the flow

* Corresponding author: lamiae.benmoussa@usmba.ac.ma

† Corresponding author: ahmed.elkhalfi@usmba.ac.ma

patterns become more complex [3]. Whereas, when the rear angle measures above 30° or falls below 10° , the swirling behavior observed affects pressure recovery and drag reduction [4]. The modification of the vortex structure reduces drag by 7 to 10% by improving the shape of the rear section [5].

This research aims to discover the optimum combination of angles which reduces drag and improves vehicle stability. This research studies flow characteristics using CFD simulations of the Ahmed body at rear angles ranging from 15° to 30° and up to 45° .

2 Methodology

2.1 Geometric details

The Catia v5r18 software was used to create an Ahmed body with real dimensions in order to perform aerodynamic tests and to improve the design characteristics of the rear part of this model. The length, width and height of the model shall be 1044 mm, 389 mm and 288 mm as shown in Fig. 1.

The different perspectives of the Ahmed body designed in the Catia v5r18 are shown in Figs. 2-4, which include isometric view, side view, front view, rear view and top view.

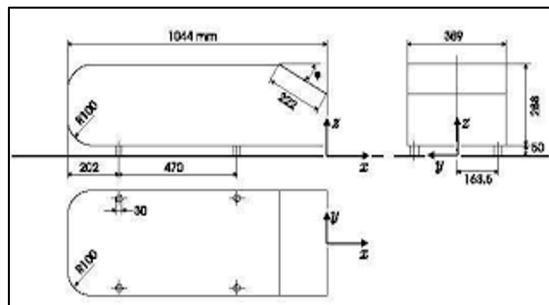


Fig. 1. Ahmed body dimensions

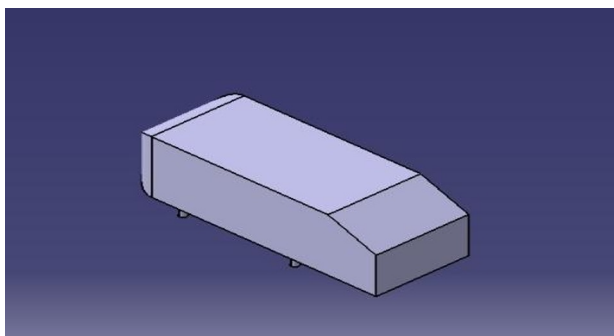


Fig. 2. Isometric view

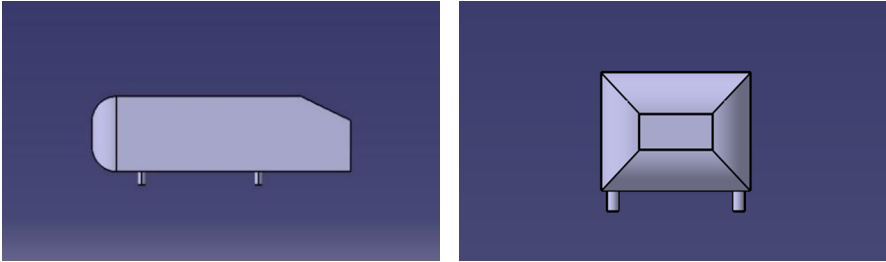


Fig. 3. Side view and Rear view

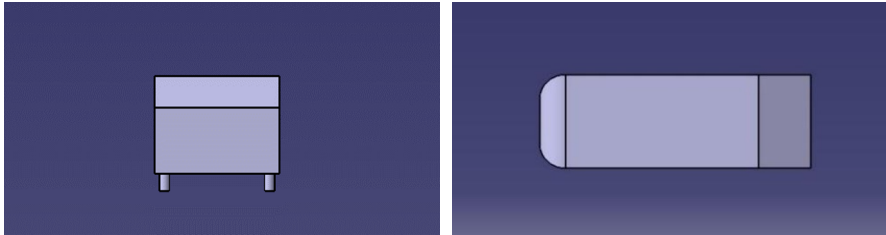


Fig. 4. Front view and Top view

3 Numerical simulation

3.1 Mesh Description

For aerodynamic simulations, 6000 mm by 800 mm by 1000 mm dimensions were used for the computational domain to make sure the flow analysis was reliable. The choice of this rectangular layout, seen in Fig. 5, was meant to ensure accurate and even flow in the domain by preventing boundary distortion effects.

Researchers improved accuracy and efficiency by simulating only one segment of the model. Skipping some details was enough since the chosen geometry is the same all the way through. From previous findings [6], [7] and [8], we find that excluding side wind help in simulations does not limit the accurate results. In fact, it makes computing faster and produces more precise meshes in the model's surroundings.

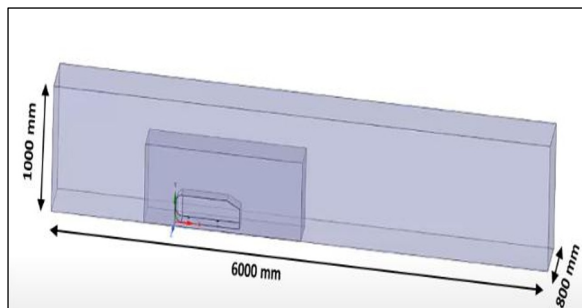


Fig. 5. Overall dimensions of computational domain

A numerical mesh and a suitable model for the aerodynamic simulation were built through the use of ANSYS Mesh Tool. It was noticed that, in the interval that was studied, the network density was lower than that defined by the limit of vehicle positions on the deck which called for more accurate results for areas where airflow would suddenly change, as illustrated in Fig. 6.

The setting up of a mesh using 973 535 nodes and 1 832 191 elements results in improved precision during numerical calculations and an accurate model of the air flow.

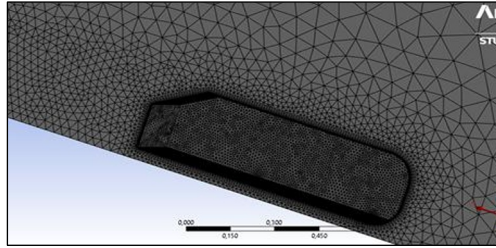


Fig. 6. Meshed model

3.2 Boundary Conditions

To get better results, this work uses the Realizable k-epsilon model, included with Realizable wall functions, to improve how the boundary layer is modeled. This model can be used in the most varied situations. Such computations mean it is suitable for applications including aerospace, automotive aerodynamics and turbomachinery.[9]

The simulation is based on three limit conditions consisting of a 30 m/s velocity inlet to simulate the impact of the front wind on the vehicle, a pressure outlet, and a moving ground set at 30 m/s. The asymmetry conditions reduce the effect of the limit, while maintaining the stability of the Ahmed model as shown in Table 1.

Table 1. Boundary Conditions

Region	Boundary conditions
Inlet	Velocity inlet: speed magnitude of 30 m/s
Outlet	Pressure outlet
Road	Moving wall: speed magnitude of 30 m/s
Top + Symmetry + Side	Symmetry (eliminating fluid/wall friction)
Body	Stationary wall

4 Results and Discussions

The rear slant angle significantly affects the performance of the Ahmed model and this is confirmed by the study of the aerodynamic coefficients. The drag coefficient is reduced to a minimum ($C_d = 0.1472$) which produces perfect stability of the airflow, and this at a rear angle of 15° which represents the best aerodynamic efficiency. The lift coefficient is 0.0942, which could help stabilize the ship, given the relatively low lift forces. The drag coefficient increases slightly at angles of 30° and 45° , while the load coefficient shows a larger increase, reaching $C_l = 0.1214$ and $C_l = 0.1325$, which may adversely affect the dynamic stability of

the vehicle. This increase in lift is due to the early separation of the surface flow, creating a low-pressure area at the rear of the vehicle. As shown in Table 2 and Fig.7.

Table 2. Total drag coefficients and lift coefficients

Value of ϕ	Drag coefficient Cd	Lift coefficient Cl
15°	0.1472	0.0942
30°	0.1568	0.1214
45°	0.1566	0.1325

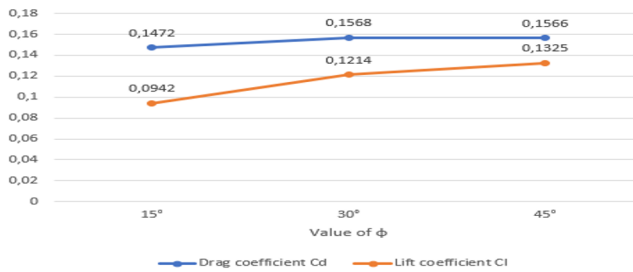


Fig. 7. drag coefficients and lift coefficients

Findings indicate that a rear slant angle of 15° provides much better aerodynamic performance than steeper alternatives. Consistent with what [10] found, these conditions reduce the low-pressure area behind the vehicle and lead to lower drag for the vehicle. The low value found for lift in our study shows that the model has a good level of dynamic stability. Similarly, [11] experiments indicate that when the rear angles are made steeper, it results in higher lift because stronger longitudinal vortices appear. Final results from [12] indicate that deflectors reduced drag slightly, but not as much as simple adjustments to the rear slant angle, proving that direct changes to the shape make a difference.

4.1 Pressure Analysis

The numerical simulation showed pressure distribution diagrams for the rear slant angles of 15°, 30° and 45° as shown in Figs. 8 to 10. This study seeks to analyse how the angle of inclination affects the airflow around the rear of a vehicle. The rear surface of the vehicle at an angle of 15° ensures a homogeneous pressure distribution as shown in Fig. 8, indicating bonded flow characteristics, which reduces flow separation and disturbances. When the vehicle is at the 30° rear tilt, presented in Figure 9, flow breaks into small parts, decreasing the pressure and causing more recirculation which might modestly affect the stability of the car. In Fig. 10, the development of the flow pattern makes it break into smaller streams at 45°, so the rear pressure grows and there is more turbulence. As a result, the vehicle experiences more lift forces and a lower level of aerodynamic performance.

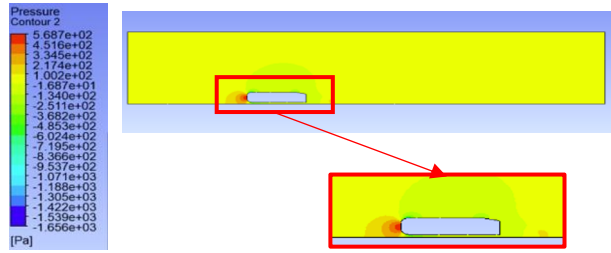


Fig. 8. Pressure on surface 15° rear slant angle.

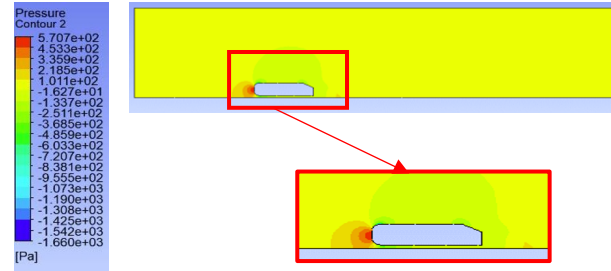


Fig. 9. Pressure on surface 30° rear slant angle.

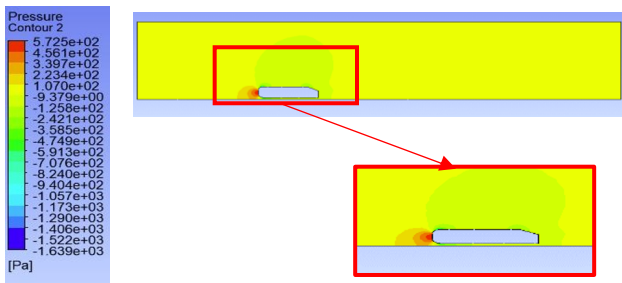


Fig. 10. Pressure on surface 45° rear slant angle.

4.2 Flow Velocity and Streamline Analysis

Figs. 11 to 13 show the distribution of the flow rate with streamlines for the three different rear angles under consideration. At an angle of 15°, the flows achieve a stable behaviour with a homogeneous distribution of velocity, which maintains the flow lines consistent and stable, indicating stable and sticky flow characteristics as shown in Fig. 11. The partial separation of the airflow leads to degradation and a gradual decrease in speed, with an angle of inclination of 30°, as shown in Fig. 12. This contributes to the formation of small air vortices and causes intermediate disturbances that affect the regularity of the flow. The 45° inclination angle shows a decrease in flow velocity due to an increase in flow separation, as shown in Fig. 13, which increases the complexity of the flow pattern resulting from significant disturbances in the flow lines.

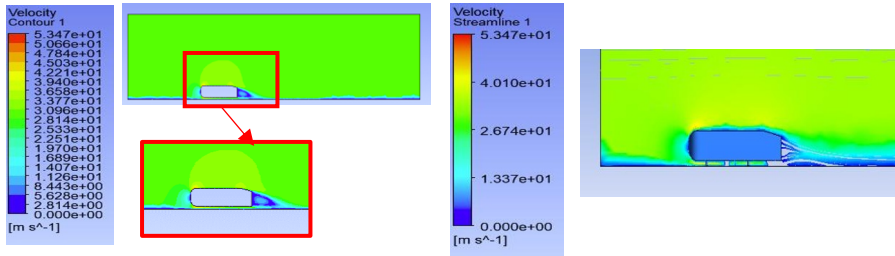


Fig. 11. Streamlines and Velocity on surface 15° rear slant angle

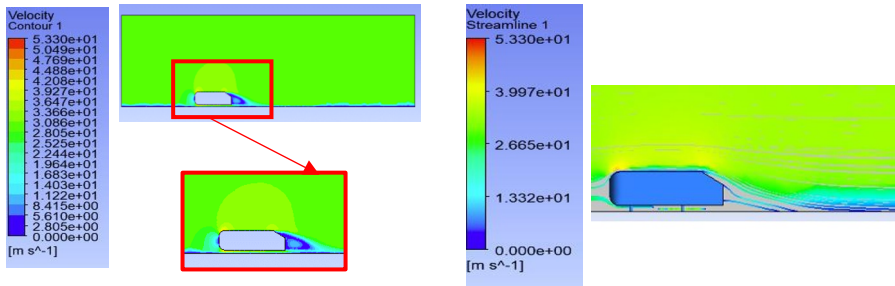


Fig. 12. Streamlines and Velocity on surface 30° rear slant angle

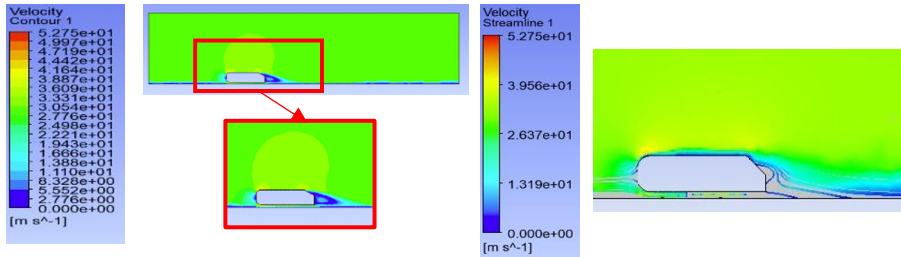


Fig. 13. Streamlines and Velocity on surface 45° rear slant angle

4.3 Evaluating Turbulent Kinetic Energy

Analyzing TKE helps to show how turbulent fluctuations are spread throughout the wake behind the Ahmed body model. Figs. 14 to 16 indicating rear slant angles of 15°, 30° and 45° demonstrate that the highest amount of TKE occurs close to the rear surface for the 15° setting. As a result, we find clearly outlined and sturdy vortices formed near the body, with most of them not moving far during the proof stage.

Simulations for slant angles of 30° and 45° indicate that the TKE spreads over a larger distance downstream. Despite lower TKE values, these conditions lead to more flow separation and increased instability in the wake which indicates weaker performance.

According to the results, a 15° rear angle ensures that the flow structure stays more consistent, thanks in part to beneficial turbulence that makes the wake more stable. A more slanted rear area spreads the turbulence out more and this makes the airplane burn more fuel during flight.

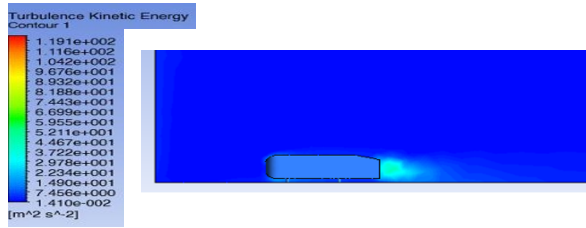


Fig. 14. Turbulence Kinetic Energy Distribution for 15° rear slant angle

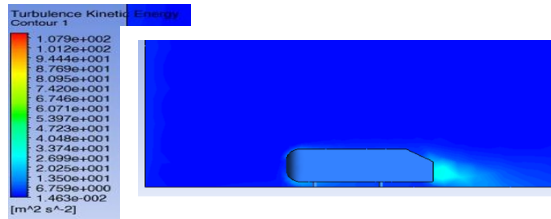


Fig. 15. Turbulence Kinetic Energy Distribution for 30° rear slant angle

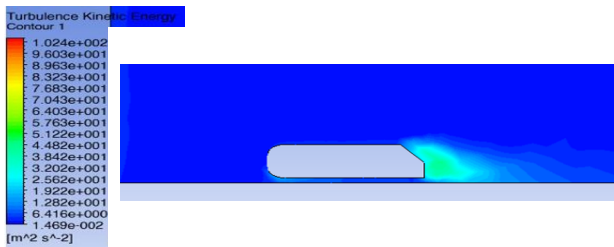


Fig. 16. Turbulence Kinetic Energy Distribution for 45° rear slant angle

5 Conclusion

The aim of this research is to analyse the aerodynamic effects of the different rear slant angles on the Ahmed body which has been adopted as a reference for the study of the aerodynamic turbulence zone behind the body to assess aerodynamic forces and rear flow characteristics, with the aim of improving industrial design by improving vehicle structures.

The experimental results showed that the adjustment of the rear angle affected the aerodynamic vortex structures, resulting in improved pressure recovery as well as a potential reduction in drag. A decrease in the rear angle of inclination of the Ahmad model from 45° to 30° and finally to 15° results in a greater decrease in the lifting force with a moderate decrease in the towing force. At an angle of 15° the drag coefficient reaches its minimum value, while vortices form in the area behind the vehicle at 30° and 45°, causing the pressure distribution and flow separation patterns to change. The simulation program ANSYS Fluent 2023R1 was used to evaluate these effects, through the regulated grid and the input speed of 30 m/s.

Such a study becomes crucial in the creation of energy-efficient engines, especially for electric cars, as every aerodynamic gain directly benefits range and reduces the car's environmental impact. Using this work, someone can find a straightforward strategy to improve car performance just by adjusting rear angle geometry, not by fitting any additional control devices. Therefore, it becomes useful for engineers in-volved in early aerodynamic design of new vehicles.

To make sure these results are accurate, more experiments must be done on the Ahmed body, both using wind tunnels and modifying parts of the airflow model. Later studies might concentrate on how crosswinds, how the flow changes on the ground or the inclusion of active flow control mechanisms influences the results.

Acknowledgment. The authors express their gratitude to the Research Laboratory in Science and Engineering at the Faculty of Science and Technology, University of Sidi Mohamed Ben Abdallah in Fes, Morocco, for their fundamental support of the research facilities and the academic environment. The PhD-Associate Scholarship - PASS program provided support for this research through the Centre National pour la Recherche Scientifique et Technique (CNRS).

References

1. S. R. Ahmed, G. Ramm, and G. Faltin, "Some Salient Features of the Time -Averaged Ground," *SAE Trans.*, vol. 93, no. 1984, pp. 473–503, 1984, [Online]. Available: [http://courses.me.metu.edu.tr/courses/me485/files/Ahmed 1984.pdf](http://courses.me.metu.edu.tr/courses/me485/files/Ahmed%201984.pdf)
2. J. Chavez, E. Vera, A. A. Martins Oliveira, and L. R. Cancino, "the Ahmed Body'S External Aerodynamics At 25° Slant Angle Rear Surface: a Numerical Analysis Using Cfd," no. January, 2020, doi: 10.26678/abcm.encit2020.cit20-0060.
3. G. Rossitto and M. E. T. D. Aérotechnique, "Giacomo ROSSITTO," 2019.
4. Y. Eulalie, "Étude aérodynamique et contrôle de la traînée sur un corps de Ahmed culot droit To cite this version : HAL Id : tel-01146911 DOCTEUR DE L ' UNIVERSITÉ DE BORDEAUX," 2015.
5. D. Govardhan, M. V. Narasimha Rao, P. Srinivasa Rao, I. Kumar, and M. Vijaya Lakshmi, "Adjoint shape optimization of Ahmed body to improve aerodynamics," *Mater. Today Proc.*, no. xxxx, 2023, doi: 10.1016/j.matpr.2023.06.410.
6. X. Hu, R. Zhang, J. Ye, X. Yan, and Z. Zhao, "Influence of different diffuser angle on Sedan's aerodynamic characteristics," *Phys. Procedia*, vol. 22, pp. 239–245, 2011, doi: 10.1016/j.phpro.2011.11.038.
7. X. J. Hu, P. Qin, P. Guo, and Y. An, "Effect of Turbulence Parameters on Numerical Simulation of Complex Automotive External Flow Field," *Appl. Mech. Mater.*, vol. 52–54, pp. 1062–1067, 2011, doi: 10.4028/WWW.SCIENTIFIC.NET/AMM.52-54.1062.
8. Hu Xingjun, Yang Bo, Wang Jing-Yu, and Li Ting, "Research on influences of rear-view mirror on aerodynamic drag characteristics of truck," *Journal of Hunan University Natural Sciences*, 2010, v37, n SUPPL. 1, p 65-69 [Online]. Available.
9. ANSYS FLUENT, "Fluent-k-epsilon," *4.4.3 Realiz. k-epsilon*, no. 12.0, pp. 12–26, 2009.
10. F. J. Bello-Millán, T. Mäkelä, L. Parras, C. del Pino, and C. Ferrera, "Experimental study on Ahmed's body drag coefficient for different yaw angles," *J. Wind Eng. Ind. Aerodyn.*, vol. 157, pp. 140–144, 2016, doi: 10.1016/j.jweia.2016.08.005.
11. F. F. Buscariolo, G. R. S. Assi, and S. J. Sherwin, "Computational study on an Ahmed Body equipped with simplified underbody diffuser," *J. Wind Eng. Ind. Aerodyn.*, vol. 209, no. October 2020, p. 104411, 2021, doi: 10.1016/j.jweia.2020.104411.

12. W. Hanfeng, Z. Yu, Z. Chao, and H. Xuhui, “Aerodynamic drag reduction of an Ahmed body based on deflectors,” *J. Wind Eng. Ind. Aerodyn.*, vol. 148, pp. 34–44, 2016, doi: 10.1016/j.jweia.2015.11.004.